Paper:
Martinez, A., Barker, J. & Di Pietro, R. (2018). Dissipative non-equilibrium Green function methodology to treat short range Coulomb interaction: current through a 1D nanostructure. *Journal of Physics: Condensed Matter, 30*(29), 294003
http://dx.doi.org/10.1088/1361-648X/aacc49

Dissipative NEGF methodology to treat short range Coulomb interaction: Current through a 1D Nanostructure

Antonio Martinez[1], John R Barker[2] and Riccardo Di Pietro[3], [1]College of Engineering, Swansea University, UK, [2]School of Engineering, University of Glasgow, UK, [3] Hitachi Cambridge Laboratory, Cambridge, UK

Abstract: A methodology describing Coulomb blockade in the Non-equilibrium Green Function formalism is presented. We carried out ballistic and dissipative simulations through a 1D quantum dot using an Einstein phonon model. Inelastic phonons with different energies have been considered. The methodology incorporates the short-range Coulomb interaction between two electrons through the use of a two-particle Green's function. Unlike previous work, the quantum dot has spatial resolution i.e. it is not just parameterized by the energy level and coupling constants of the dot. Our method intends to describe the effect of electron localization while maintaining an open boundary or extended wave function. The formalism conserves the current through the nanostructure. A simple 1D model is used to explain the increase of mobility in semi-crystalline polymers as a function of the electron concentration. The mechanism suggested is based on the lifting of energy levels into the transmission window as a result of the local electron-electron repulsion inside a crystalline domain. The results are aligned with recent experimental findings. Finally, as a proof of concept, we present a simulation of a low temperature resonant structure showing the stability diagram in the Coulomb blockade regime.

.

1. Introduction

The Non Equilibrium Green Function formalism (NEGF) **[1]** has been extensively used to describe electron transport through nanotransistors **[2]** and other quantum nanostructures **[3].** Ballistic and dissipative calculations have been carried for V and III-V materials and various device structures **[4].** Carrier transport through quantum dots has also been thoroughly investigated using the NEGF formalism. In general, transport equations and Poisson equation need to be solved in order to calculate the current through the transistor device. Usually, the electrostatic potential calculated from the Poisson equation is used as the potential energy of the electron and is entered into the Schrodinger equation to calculate the transmission or current. This so-called mean field approximation fails when few electrons are localized or pass through very small regions such as quantum dots of few nanometre across. Coulomb blockade (CB) **[5]** and Kondo effect **[6-7]** are phenomena showing a breakdown of the mean field approximation. The role of local Coulomb interaction in narrow band gap materials was first studied by Hubbard **[8]**. He wrote a minimal Hamiltonian in order to treat the penalty paid by electrons when localized close to each other. He proved that for certain cases this interaction energy decayed very quickly as the distance between electrons increases. This could be represented by a constant term when the electrons occupied the same atom or molecule and zero when the electron where in different atoms. So this interaction energy will in general depend on the extra population of electrons in the atom or small nanostructure and the localization of the electron or overlap of the single electron wave functions **[8].** Wingreen *et al* **[9]** studied the Coulomb blockade in an open nanostructure using a simplified Hubbard Hamiltonian: the Anderson model **[10]**. Their paper

used the Schrödinger equation in concomitance with a kinetic equation for the distribution function i.e NEGF formalism. They were able to reproduce certain experimental features. Pals and MacKinnon **[11]** also carried out NEGF simulations for single and double quantum dots using the Anderson model; they demonstrated negative differential resistance using this model. Recently, Ryndyk and Cunniverti **[12]** used a more general kinetic equation to describe the Coulomb blockade in single and double quantum dots, however, their calculations did not consider the electron-phonon interaction. Song **[13]** extended this description to molecules but used the Wingreen model **[9]** and demonstrated that the modification in the kinetic equation can be neglected for certain cases. Another refinement of Wingreen's model was used by Zimboskaya to study Quantum Dot (QD) populations, conductance **[14]** and thermovoltage **[15].** However, all the afore-mentioned models assumed the QD to be *featureless* so it is described in the formalism by the energy levels only and the connection with the environment is given by coupling constants representing the transmission between the dot and the contacts. In the present work the dot is described in a spatial representation and has a *spatial dimension and potential shape*. In addition, the dot is described as a quasi-resonant structure, and energy levels are *derived* from the resonant structure. Electrons enter the dot through tunnelling barriers. Our formulation is more aligned with the usual spatial description of the NEGF device simulation of nanotransistors in which the shape of the nanostructure, the height and width of the contact barrier plays a crucial role. In addition, we included in our description the local Coulomb energy through a *two-particle* Green function (2pGF). The Coulomb energy can be calculated from the overlap of the single electron wavefunction as done by Hubbard **[8].** We have calculated the current through a 1D resonant nanostructure. We compared the currents obtained by the inclusion and exclusion of the two particle Green function. We have also carried out dissipative simulations using a simplified Einstein phonon model. We have compared elastic and inelastic processes and also different strengths of interactions. Our result seems to support the claim in **[16]** that the inter-electron Coulomb repulsion is responsible for the increases in mobility observed in semi-crystalline polymers. The nanostructure considered here has the same dimensions as one of the crystalline domains studied in **[16]** and our Coulomb energy is calculated using the polymer dielectric constant. Section 1 introduces the equations, models and the nanostructure. Section 2 presents and analyses the results. Finally, conclusions and future work are drawn in the last section.

The formalism treats the electron transport quantum mechanically and the electron distribution function is assumed Fermi-Dirac in the contact or large reservoir at constant potential. Due to the non-equilibrium conditions (electric fields) the electron distribution function is calculated inside the device due to the balance between phonon and electron energy exchange.

2. Methodology

In this section, we present a method to include local Coulomb interaction in a spatially resolved NEGF formalism. Spatially resolved means that the equations involved need to be discretised in the simulation domain such as a device (or Quantum Dot) and its contact regions. In this work we used an effective mass Hamiltonian to describe the electrons in the material. We will not derive the equations here but refer the reader to the appropriate literature **[7, 12 and 14]**. However, we will *briefly* indicate the steps involved. We start with the second-quantised Hamiltonian including the electron-electron interaction and utilise the Heisenberg equations of motion. The latter are used to write an equation for the expectation values of product of creation and annihilation operators. This produces a linked infinite hierarchy of equations connecting the *one particle* Green function (GF) with the *two particle* GF, and with three particles GF and so

on. At this point a truncation approximation must be made to reduce the infinite system to a finite system of equations. Usually, the equation for a single particle Green function contains a two-particle Green function. Approximating the two-particle Green function by a product of single particle Green functions allows the reduction of the whole system to just one equation. Alternatively, in the equation of the two-particle Green function, one may approximate the three particle Green function as a function of a two particle Green function and a one particle Green function. This will produce a coupled set of equations for the one and two-particle Green functions. The idea is that the inclusion of the local Coulomb interaction may be achieved by considering just the two-particle GF. The way to include the two particle Green function is not universal and depends on which phenomena are to be described. The equations used in the present work are sufficient to describe Coulomb blockade and the phenomena of current enhancement due to Coulomb repulsion observed in polymers but they are *insufficient* to describe the Kondo effect. However, our simulations are mainly for room temperature with the exception of a simulation of a resonant structure at low temperature (15 K) to demonstrate Coulomb blockade.

The Green Function Matrix (they are matrices in the spatial index but the indexes are not shown) equations considered are **[9]**:

$$(E - H - \Sigma_\sigma^R)G_\sigma^R = I + UG_\sigma^2 \quad (1)$$

$$(E - H - \Sigma_\sigma^R - U)G_\sigma^2 = n_{-\sigma} \quad (2)$$

$$G_\sigma^< = G_\sigma^R \Sigma_\sigma^< G_\sigma^A \quad (3)$$

The first equation represents the dynamics (it is similar to a Schrödinger equation) for the retarded Green function $G^R{}_\sigma$ (the upper index *R* stand for retarded). The sub index σ, describes the two possible spin orientations (up, down) of an electron. Thus each orientation requires an equation of motion. The *E, H* and Σ^R terms denote the energy, Hamiltonian (without the local Coulomb interaction but including the potential energy of the nanostructure) and retarded self-energy respectively. An expression for the Hamiltonian with the local interaction included is described in Appendix A, equation (A1). The second term in the right hand side contains the effect of the local Coulomb repulsion through the Coulomb energy *U* and the two-particle Green function $G^2{}_\sigma$. The second equation is an equation to calculate the two-particle Green function where the term $n_{-\sigma}$ represents the number of electrons in the dot with spin opposite to σ. Finally, the third equation is the kinetic equation to calculate the lesser Green function $G^<{}_\sigma$; it contains the total lesser self-energy. The latter is proportional to the scattering rates and has two parts, one related to the contacts (assumed in equilibrium) and the other to the scattering mechanism inside the device (as phonon scattering). In this work, the Hamiltonian and the boundary condition are spin independent so $n_{-\sigma} = n_\sigma$.

Appendix A makes plausible the ideas behind the derivation of equations (1) and (2). The derivations are well documented in several textbooks **[7, 17, 18].** Essentially, equations (1) and (2) are exact for an *isolated* dot i.e. if the self-energies of the contacts are removed from both equations. If we coupled the dot with the contacts, contact self-energies and other Green Functions will appears in equations (1) and (2). These self-energies, in principle, are dependent on *U* and are formed by the addition of many terms. If instead of these self-energies, we used only the self-energies that appear in the problem when *U*=0 (i.e. a *non-interacting* dot but

coupled to the leads), we recover equations (1) and (2) used in the present paper and used by many other authors **[5, 7, 17, 18, 19].** It could be said that they are the simplest approximation that produces Coulomb blockade within NEGF formalism. A simplified description of the derivation is found in **[7]**.

3. Results

We have used the above methodology to calculate the current through a simple 1D nanostructure. The length of the resonant structure is about 7nm (estimated by the local density of states in the well), which is in agreement with some of the lengths of the crystalline islands in **[16]**. The magnitude of the source-channel barrier is approximately 100 meV similar to those assumed in **[16].** In this work, the short-range Coulomb energy U **[8]** is assumed to be 100 meV for the case of two electrons occupying the nanostructure. This value may be estimated from the Coulomb integral **[8]** in the well for the two opposite spin electrons. A heuristic quantum mechanical calculation using the two-centre integrals **[20]** with a dielectric constant of 3 and using Gaussian functions produces a value U= 80 meV for a spherical cavity of approximate 7 nm in diameter. The electrostatic Coulomb interaction energy between two electrons at 7 nm apart is approximately U = 70 meV. The above values show an indication of the order of magnitude of this interaction.

Our simulations illustrate that inclusion of the Coulomb interaction leads to a substantial enhancement in the current and that the increase is still there when scattering is considered. This makes plausible the arguments of paper **[16]** that the Coulomb interaction in the semi-crystalline polymer enhances the charge transport.

Equations (1-3) are solved self-consistently for a double barrier nanostructure mimicking one of the nanocrystallite of reference 16 . We used a spatial resolved mesh of 0.1 Angstroms and in an energy mesh of 0.1 meV. Ballistic and dissipative (phonon scattering) current calculations have been carried out using a simple inelastic phonon scattering mechanism (Einstein model). The corresponding ***self-energies*** **[7, 17, 21,22,23,24]** are calculated using the self-consistent Born approximation **[17, 21 (Appendix), 25, 26]** and the explicit expressions are given in Appendix A2.

The inelastic phonon energies used in this work is **6 meV, 10 meV and 12 meV**. Our main goals are: to compare the impact on the current from the local Coulomb repulsion; and also to study the effect of phonon scattering. In our simulations the difference between the two Fermi levels is kept constant but the Fermi levels are raised relative to the 1D structure. Our intention is to mimic an increase of electron population inside the nanostructure as in **[16].**

Fig. 1 shows the local density of states (LDOS) with and without considering the 2pGF, when the total electron occupation in the well is 2 (1 for each spin direction). The white line represents the electrostatic potential energy seen by the electron and therefore outlines the resonant structure. The density of states is mainly localized in the nanostructure and in the contact but not inside the barriers; this indicates the quasi-localization of the electron inside the well. However, the second energy level of the well shows a large penetration into the barrier as seen in figure 1. This penetration also allows for a lowering in the energy level with respect to the isolated dot, *an effect that cannot be considered if a spatial description of the dot is missing*.

When the 2pGF is neglected, the ground state energy of the electron inside the cavity is lower than the source potential energy. In addition the next confined state energy is too high in energy to be occupied. This is because the occupation is decreased by a Boltzmann factor relative to the ground state energy. In this case electron current through the nanostructure is expected to be small, as electrons have no quasi-resonant level to connect the right and left contact. However, the inclusion of the local electron-electron interaction through the 2pGF (upper panel of Fig. 2) causes the energy levels to shift upwards in the cavity allowing the ground state of the well to enter into the energy window connecting the two contacts and a quasi-resonant level is established. In this case, current can flow more easily and the current is enhanced substantially reaching a maximum of **200 % at 130mV** but dropping to **100 %** when the cavity is occupied. This is shown in **Fig. 2**, which depicts the current as a function of the bias for the cases when the 2pGF is considered or not. This figure also shows the effect of the scattering on the current. The scattering reduces the current by scattering the electrons backwards. The current reduction is **35%** when the 2pGF is considered and **5 %** otherwise. The large impact of scattering when 2pGF is considered is due to the scattering of electrons to lower energy levels making the probability of transmission through the second barrier lower. This is observed in **Fig. 3,** which shows the current spectra along the structure when 2pGF is included.
The figure also shows that the current spectrum is continuous through the nanostructure, the maximum deviation $\Delta I / I_{av}$ of the current along the nanostructure from the average current I_{av} is 0.01. Therefore, the current is conserved locally. In order to get a better error the number of Born iterations needs to be increased. In addition, it is important to note that the LDOS shows the two poles related to the 1 or 2 electron occupation, both poles are shown at an intermediate occupation number.
In order to understand the role played by Coulomb repulsion in the transport of the electrons through the nanostructure, it is better to look at **Fig 4,** which shows the normalized spectrum of the current (the current per unit energy and divided by the total current) at different bias or different occupation of the well. This figure shows how the current distributes in two peaks on the energy axis for each bias. The low energy peak corresponds to the energy shift induced by the Coulomb repulsion and the higher is the second energy level of the well. At very low voltages the electron occupation in the well is low and the second peak controls the transport. This can be seen in **Fig. 5**, which shows the electron occupation in the well as a function of the bias. As the occupation of the well increases, the current start to be controlled by the Coulomb repulsion energy level. It should be noted that the importance of Coulomb repulsion appears very early due to the fact that the population of the electrons decay exponentially with increasing energy so only a few electrons in the source have access to the second level. However at very low occupations, the local DOS of the Coulomb level is very small and the second energy level of the well dominates.

Fig 6 and 7 show the LDOS for 10^{-3} eV^2 and 10^{-2} eV^2 electron-phonon couplings. Note the increase in broadening as the coupling constant increases.

We have also considered the impact on the current for different phonon energies. **Fig. 8** depicts the current voltage characteristic for 6meV, 10meV and 12 meV phonon energies. For successively larger phonon energies the current increases as the density of the states is concentrate around the quasi-resonant state. An additional reason for the increasing of current with increasing phonon energy is the fact that as electrons are scatter down the well the probability to be reflected back to the source is reduced.

Finally, to confirm that our formalism reproduces the Coulomb blockade, we have carried out calculations for low temperature: 15K. The nanostructure is similar to those which have been analysed early however with relatively thicker walls and a smaller width. **Fig. 9** shows the nanostructure, the energy for one electron and for two-electron in the well (i.e. the *U* shifted ground state). The height of the barrier is 1eV. **Fig. 10** shows part of the Coulomb blockade stability diagram i.e. the conductance plotted in the V_G-V_D diagram. Our results agree with those using a non-structured dot. Ref (12 and 13) Note that the distance between the two vertices in the horizontal is equal to the charging energy *U* as expected.

4. Conclusions

The present study demonstrates that many-electron effects similar to the Coulomb blockade can be integrated in a phenomenological way into the standard *position-dependent* NEGF formalism of quantum transport in nanostructures that until now has focussed on the *single-particle* formalism. Our introduction of two-particle Green functions for describing electron-electron coupling in a *spatially resolved* resonant structure is an important advance in quantum transport modelling for nanostructures. Because of the spatial extension of the structure the potential inside the structure may vary spatially. In addition, the self-consistent position-dependent potential may control the size and height of the barriers bounding the nanostructure. However, the issue of how to address the transition between localization and delocalization of electrons inside an open nanostructure remains unsolved, as is the self-consistent calculation of the local Coulomb interaction in an open nanostructure. It is noted that the extension to full 3D models leads to significant computational complexity.

Our calculations, when applied to a particular 1D model nanostructure, demonstrated a current increase when the 2pGF was incorporated. This is due to the shift and splitting of the energy levels caused by electron repulsion inside the structure. Applying this qualitative result to experimental observations on polycrystalline polymers suggests the increase in current will result in an increase of observed mobility and supports the hypothesis that electron-electron interaction could be responsible for the mobility increase in nano-crystallites **[16].** In addition, the enhancement in current due to the 2pGF is smaller when phonon scattering is considered. However, the impact of scattering in the current voltage characteristic is diminished when the 2pGF is considered.

Finally, simulations of a double barrier at low temperature showed as a proof of concept that our formalism is able to produce the stability diagram (Coulomb diamond) under Coulomb blockade conditions. This fact confirms the possibility in the future to carry out quantum transport simulation of nano-devices beyond the orthodox theory using two-particle space-dependent Green functions. Future work on modelling realistic nano-transistors will require the incorporation of self-consistent electrostatics.

Appendix A

The total Hamiltonian includes the effective mass Hamiltonian and the local Coulomb repulsion U interaction inside the dot (the i index runs through the dot and the contacts)

$$H_T = \frac{-\hbar^2}{2m^*\Delta x^2}\sum_{i,\sigma}(a^+_{i-1,\sigma}a_{i,\sigma} + a^+_{i+1,\sigma}a_{i,\sigma} - 2a^+_{i,\sigma}a_{i,\sigma}) + \ldots$$

$$+\sum_{i,\sigma} U_{Dot}(i)a^+_{i,\sigma}a_{i,\sigma} + U\sum_{i\in Dot} a^+_{i,\uparrow}a_{i,\uparrow}\, a^+_{i,\downarrow}a_{i,\downarrow} \qquad \text{A1}$$

The first term is the kinetic energy in the effective mass approximation (Δx being the discretisation mesh), the second is the potential due to the nanostructure and the third is the Hubbard Coulomb repulsion, i denotes the spatial discretisation index along the 1D nanostructure. U_{Dot} (i) is the potential energy due to the nanostructure. The U interaction is considered only inside the dot.

Einstein Phonons: The phonon model used here is described in references [17, 21, 22, 23 and 24] and it is assumed to be *local*, i.e. the derived self-energies are diagonal in the space index i. The self-energies associated to electron phonon interaction are given by [17, 21 and 23]:

$$\Sigma^<_\sigma(i,i,\varepsilon) = D(n_{ph}+1)G^<_\sigma\big(i,i,\varepsilon+\varepsilon_{ph}\big) + Dn_{ph}G^>_\sigma(i,i,\varepsilon-\varepsilon_{ph}) \qquad \text{A2}$$

$$\Sigma^>_\sigma(i,i,\varepsilon) = D(n_{ph}+1)G^>_\sigma\big(i,i,\varepsilon-\varepsilon_{ph}\big) + Dn_{ph}G^<_\sigma(i,i,\varepsilon+\varepsilon_{ph}) \qquad \text{A3}$$

$$\Sigma^R_\sigma = \text{i Imag}\,(\Sigma^>_\sigma - \Sigma^<_\sigma)/2 \qquad \text{A4}$$

Where D , ε_{ph} and n_{ph} is the electron phonon coupling, the phonon energy, and the Bose Einstein distribution function respectively. D and ε_{ph} are assumed constants Ref [23, 24]. $G^<$ and $G^>$ the lesser and greater green function respectively.

Derivation of Eqs for G^R and G^2, references and books:

In principle, Eq 1 and 2 are derived elsewhere; see the references mentioned below, which contain several textbooks. We have dropped the spatial indexes here as the dot has only one site and because they do not play any role in the derivation. The definitions of the G^R and G^2 are found elsewhere [17, 18, 19] and are given by:

$$G^R_\sigma(t,t') = -i\theta(t-t')\langle\{a_\sigma(t), a^+_\sigma(t')\}\rangle \qquad \text{A5}$$

$$G^2_\sigma(t,t') = -i\theta(t-t')\langle\{a_\sigma(t)a^\pm_{\bar\sigma}(t)a_{\bar\sigma}(t), a^+_\sigma(t')\}\rangle \qquad \text{A6}$$

The $< >$ is a trace for all the expectation values of the non-equilibrium states of the system and {,} is the anti-commutator for Fermions.

The equations for GR and G2 for an isolated dot (i.e. with no contacts) in the Fourier space can be derived from the Heisenberg equation of motion

$$i\dot{a_\sigma} = [a_\sigma, H] \qquad \text{A8}$$

Where the dot indicates time derivative and the Hamiltonian for an interacting dot is given by:

$$H = \sum_\sigma \varepsilon_\sigma a_\sigma^+ a_\sigma + U a_\uparrow^+ a_\uparrow a_\downarrow^+ a_\downarrow \qquad \text{A9}$$

using equation A8 and the definitions A5 and A6; and after a lengthy algebra of anti-commutators the following equations for the green functions are obtained.

$$(\varepsilon - \varepsilon_\sigma) G_\sigma^R(\varepsilon) = 1 + U G_\sigma^2(\varepsilon) \qquad \text{A10}$$

$$(\varepsilon - \varepsilon_\sigma - U) G_\sigma^2(\varepsilon) = n_{-\sigma} \qquad \text{A11}$$

These equations are similar to the equations in this paper with only the coupling with the contact missing. Therefore the approximations used in this paper and in references [17 , 18, and 19] introduce the contact self-energies obtained for the non-interacting system (i.e. no Coulomb interaction). This approximation excludes the Kondo effect as has been pointed out in [7 , 17]. The above equations produce the ε_σ and $\varepsilon_\sigma + U$ poles in the local density of states as required for Coulomb blockade.

References

[1] Keldysh LV,Sov, Phys, JETP, 20 1018 (1965)
[2] A. Svizhenko et al J. Appl. Phys 91, 2343, (2002)
[3] A. Martinez et al. IEEE Transactions on Electron Devices, 54(9), pp. 2213-2222. (2007)
[4] A. Price et al "Electrothermal simulations of Si and III-V nanowire field effect transistors: A non-equilibrium Green's function study", Journal of Applied Physics 122, 074502 (2017);
[5] Y. Meir, N. S. Wingreen, and P. A. Lee, Phys. Rev. Lett. 66, 3048 (1991).
[6] J. Kondo, Jun. "Resistance Minimum in Dilute Magnetic Alloys". Progress of Theoretical Physics. 32: 37 (964).
[7] S. Datta, Quantum Transport: Atom to Transistor (Cambridge University Press, Cambridge, England), 2005.
[8] J. Hubbard, Proc. Roy. Soc. A 276, 238 (1963)
[9] Y. Meir, N. S. Wingreen, and P. A. Lee, Phys. Rev. Lett. 70, 2601 (1993).
[10] Anderson P W 1961 Phys. Rev. 124 41
[11] P. Pals and A. MacKinnon, J. Phys.: Condens. Matter 8, 5401 (1996).
[12] B. Song, D. A Ryndyk and Cuniberti, Phys Rev. B 76,045408, (2007)

[13] B. Song, DFT-based calculation of Coulomb blockade in molecular junction, arXiv:0710.0475 (2007)
[14] N. A. Zimbovskaya, "Electron transport through a quantum dot in the Coulomb blockade regime: Nonequilibrium Green's function based model", Phys. Rev. B 78, 035331
[15] N. A. Zimbovskaya, Seebeck effect in molecular junctions, Journal of Physics: Condensed Matter 28 (18), 183002. The effect of Coulomb interactions on nonlinear thermovoltage and thermocurrent in quantum dots, J. Chem. Phys. 142, 244310 (2015).

[16] R. Di Pietro, I. Nasrallah, J. Carpenter, E. Gann, L. S. Kolln, L. Thomsen, D. Venkateshvaran, K. O'hara, A. Sadhanala, M. Chabinyc, C. R. Mcneill, A. Facchetti, H. Ade, H. Sirringhaus, and D. Neher, "Coulomb Enhanced Charge Transport in Semicrystalline Polymer Semiconductors", Adv. Funct. Mater. 28, 28, 1 (2016),

[17] Quantum Kinetics in Transport and Optics of Semiconductors, Hartmut Haug, Antti-Pekka Jauho, Springer Berlin Heidelberg, (1998), chapter 12.

[18] Green's functions and condensed matter, G. Rickayzen, Academic Press, (1980). Chapter 10.

[19] Energy Transfer Dynamics in Biomaterial Systems, springer verlag pag, 209 edited by Irene Burghardt, "Green Function Techniques in the Treatment of Quantum Transport at the Molecular Scale" D. A. Ryndyk, R. Gutierrez, B. Song, and G. Cuniberti

[20] Slater, J. C. Quantum Theory of Molecules and Solids, Vol. 1: Electronic structure of molecules. New York: McGraw-Hill, 1963-74.

[21] Impact of phonon scattering in Si/GaAs/InGaAs nanowires and FinFets: a NEGF perspective, Martinez, A., Price, A., Valin, R. Manuel Aldegunde and John Barker. J Comput Electron (2016) 15: 1130. https://doi.org/10.1007/s10825-016-0851-0

[22] "Nonequilibrium Green's-function method applied to double-barrier resonant-tunneling diodes" R. Lake and S. Datta *Phys. Rev. B 45, 6670 – (1992), eq. 10*

**[23] "A simple kinetic equation for steady-state quantum transport"
S. Datta, J. Phys. Condens. Matter 2, 8023 (1990).**

[24] "Nonequilibrium Green's function based models for dephasing in quantum transport", R. Golizadeh-Mojarad and S. Datta, Phys. Rev. B 75, 081301 (2007)

**[25]"Self-energy Models for Scattering in Semiconductor Nanoscale Devices: Causality Considerations and the Spectral Sum Rule",
John R Barker, and Antonio Martinez,
Material Research Society Proceedings, MRS Online Proceedings Library, volume** 1551**, 17-22 (2013)**

[26] "Causal self-energies for NEGF modelling of quantum nano-wires"
John R. Barker, Antonio Martinez, Manuel Aldegunde and Raul Valin
Journal of Physics: Conference Series **526**, 012001 (2014).

Figures

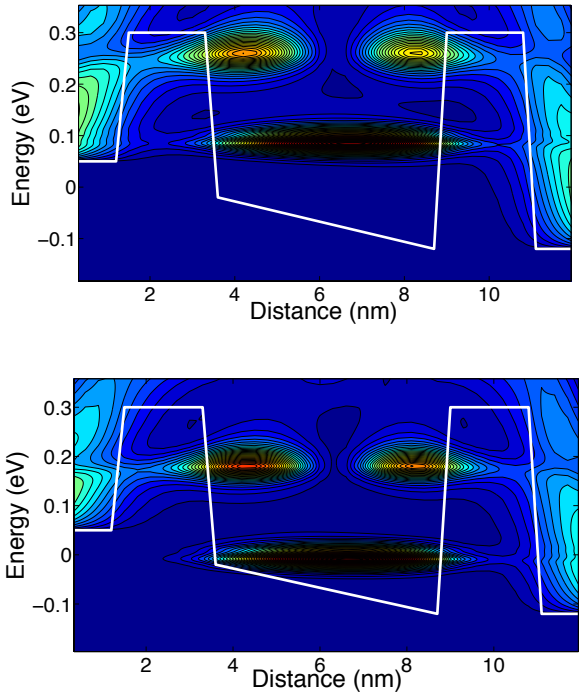

Fig.1 Upper panel: The LDOS including 2pGF. Lower panel: The LDOS without considering the 2pGF, when the electron occupation in the well is 2.

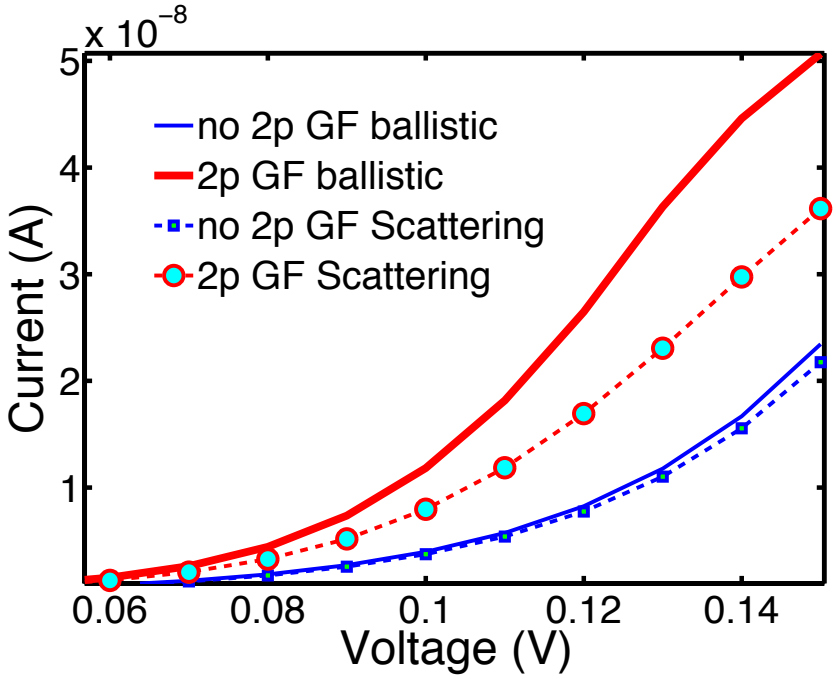

Fig.2 The current voltage characteristics for ballistic and scattering simulations. The simulations shown in red include the 2pGF and the blue neglects it.

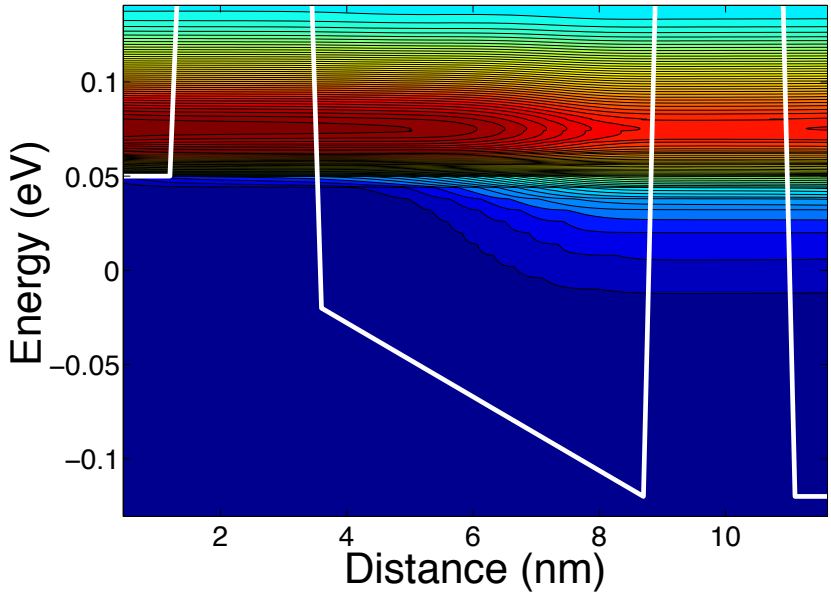

Fig 3. Current spectra through the nanostructure. The current is continuous through the structure and spread towards the right due to the inelastic scattering. The broadening of the distribution on the drain is due to inelastic phonon scattering.

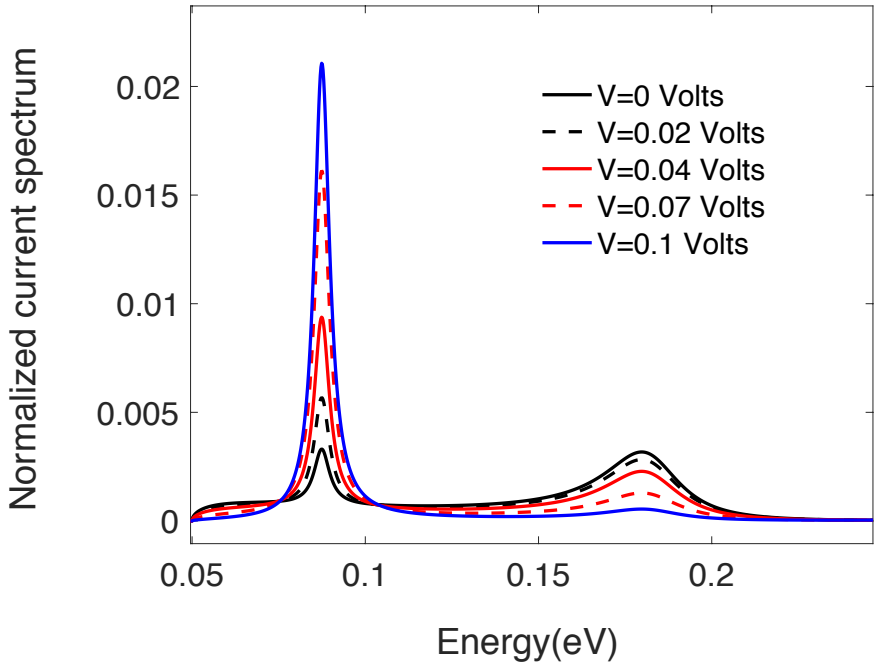

Fig. 4. The normalized current spectrum (when 2pGF is considered) for different voltages and considering ballistic transport.

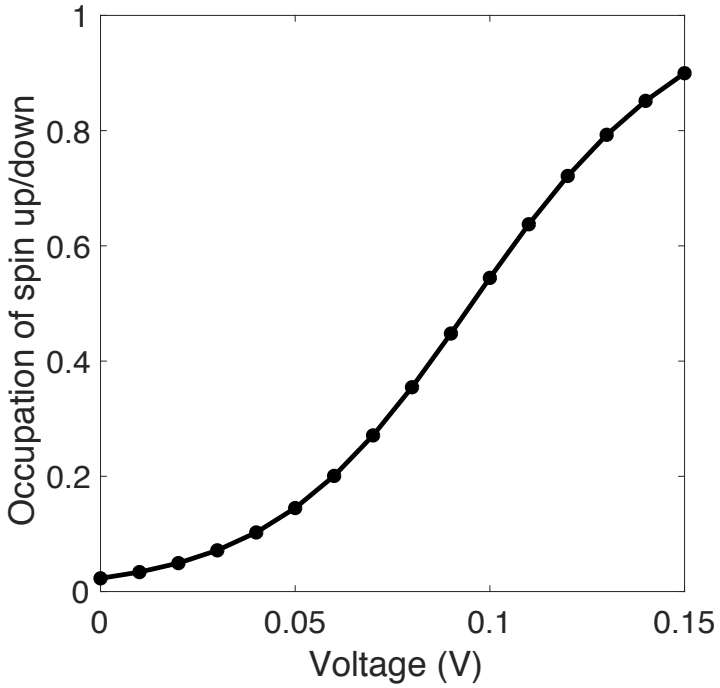

Fig. 5. Occupation of the electron with spin up or down in the well

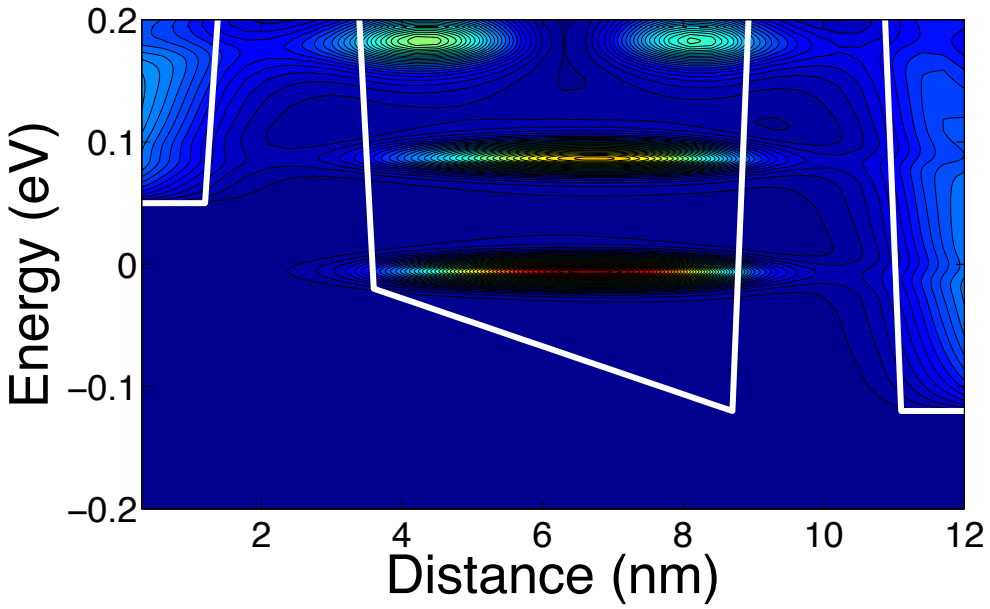

Fig. 6 LDOS for intermediate well occupation (0<occupation<2). For an electron interaction coupling strength of $0.001eV^2$. The two poles of the LDOS are shown simultaneously in the GR function.

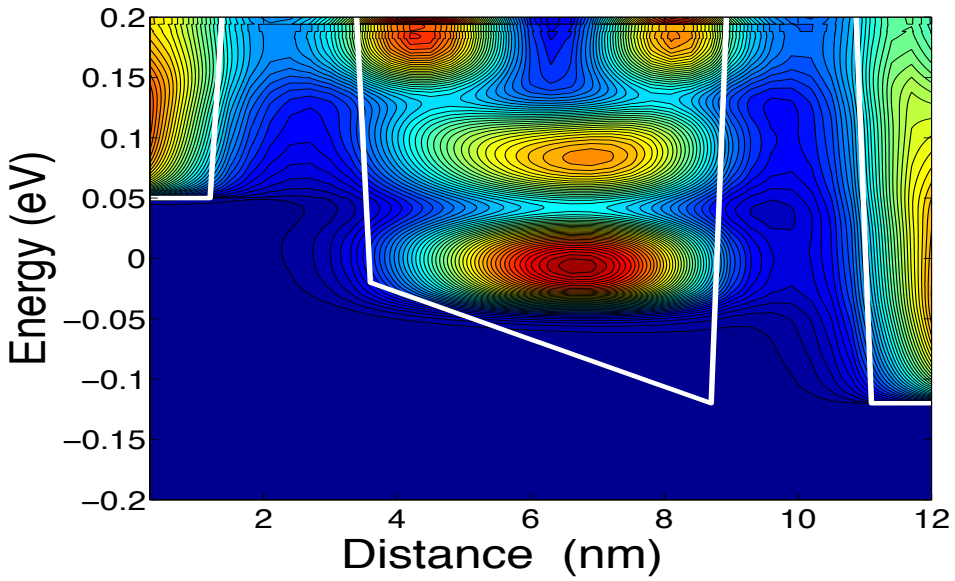

Fig. 7. LDOS for intermediate well occupation (0<occupation<2). For an electron interaction coupling strength of $0.01eV^{2}$. The large broadening of the energy levels are a result of strong electron-phonon coupling

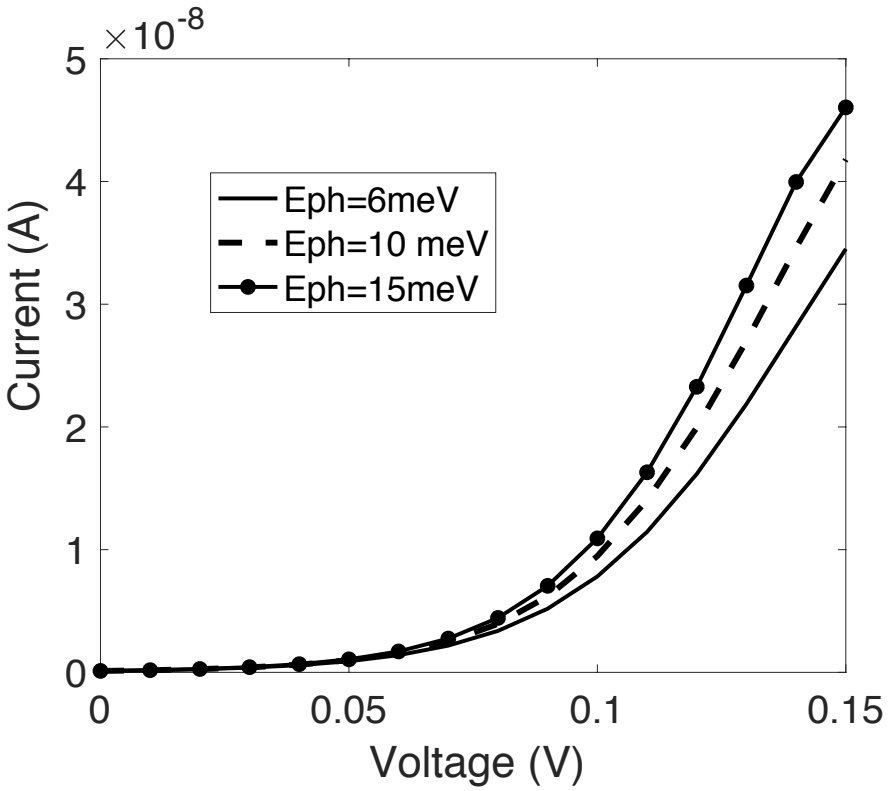

Fig. 8 The current voltage characteristics for different phonons energies including 2pGF.

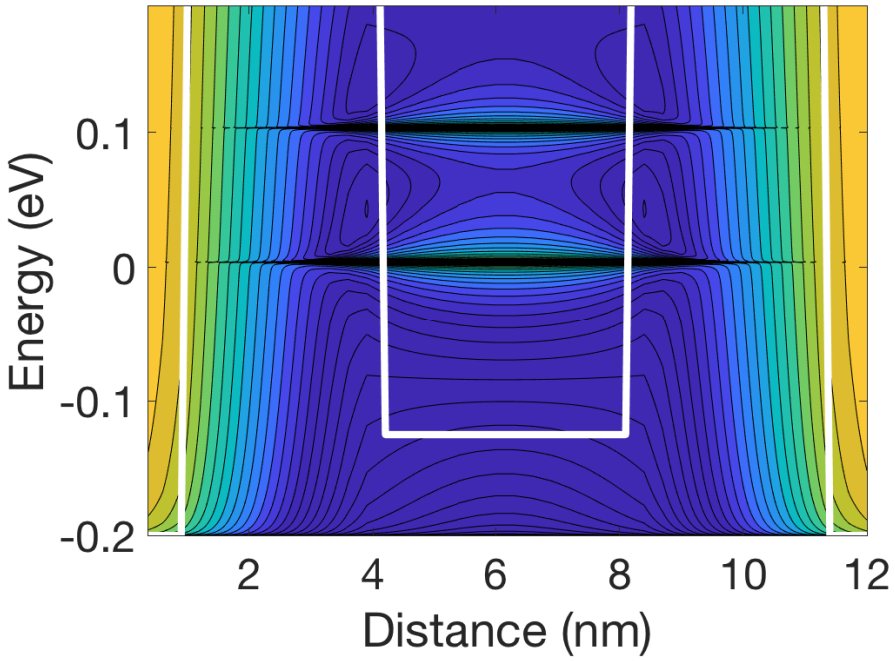

Fig. 9. LDOS showing the ground state for one and two electrons inside the structure. The nanostructure potential is shown in white.

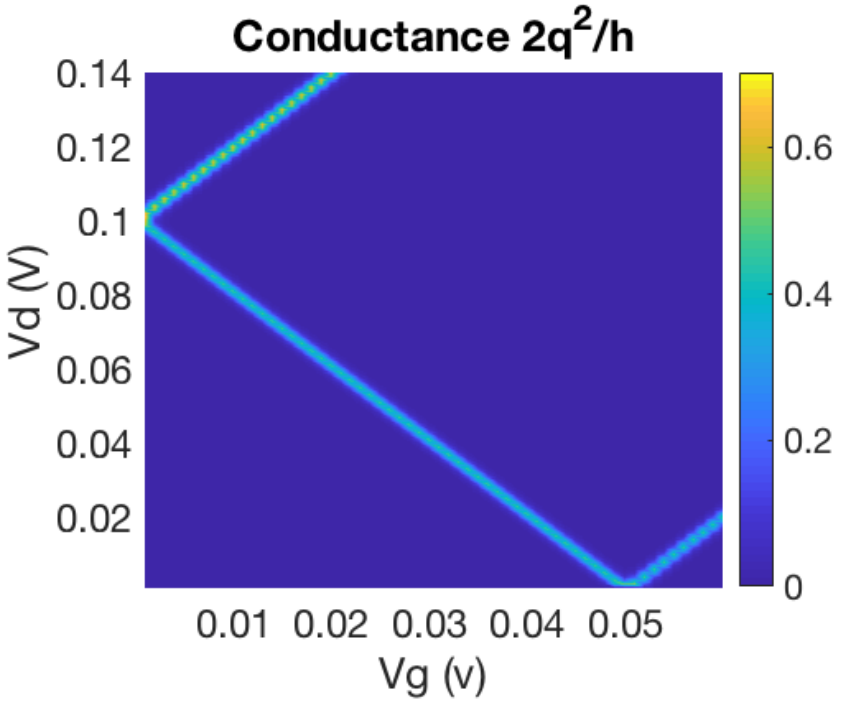

Fig. 10. Conductance as a function of gate and drain bias. Only part of the Coulomb Blockade stability diagram is shown.